Stem Cell Research 24 (2017) 61-68

Title

Small molecule AT7867 proliferates PDX1-expressing pancreatic progenitor cells derived from human pluripotent stem cells

Authors

Azuma Kimura[1], Taro Toyoda[1], Yohei Nishi[1], Makoto Nasu[1], Akira Ohta[1] and Kenji Osafune[1]

[1]Center for iPS Cell Research and Application (CiRA), Kyoto University, 53 Kawahara-cho, Shogoin, Sakyo-ku, Kyoto 606-8507, Japan

Contact information

Kenji Osafune
53 Kawahara-cho, Shogoin, Sakyo-ku, Kyoto 606-8507, Japan
Tel: +81-75-366-7058; Fax: +81-75-366-7077
osafu@cira.kyoto-u.ac.jp

Taro Toyoda
53 Kawahara-cho, Shogoin, Sakyo-ku, Kyoto 606-8507, Japan
Tel: +81-75-366-7058; Fax: +81-75-366-7077
t.toyoda@cira.kyoto-u.ac.jp

The final publication is available at https://doi.org/10.1016/j.scr.2017.08.010.

Abstract

While pancreatic islet transplantation achieves insulin independence in type 1 diabetes (T1D) patients, its widespread application is limited by donor tissue scarcity. Pancreatic progenitor cells (PPCs) give rise to all cell types in the pancreas during development. PPCs derived from human pluripotent stem cells have been shown to differentiate into functional β cells both *in vitro* and *in vivo*, and to reverse hyperglycemia, at least in mice. Therefore, PPCs have great potential to serve as an alternative cell source for cell therapy, and the identification of compounds that facilitate PPC proliferation could provide stable and large-scale pancreatic cell preparation systems in clinical settings. Here, we developed and performed cell-based screens to identify small molecules that induce the proliferation of hiPSC-derived PDX1-expressing PPCs. The screening identified AT7867, which promoted PPC proliferation approximately five-fold within six days through the maintenance of a high $Ki67^+$ cell ratio. The induced proliferation by AT7867 does not result in DNA damage, as revealed by pHH2AX staining, and is observed specifically in PPCs but not other cell types. The established platform utilizing small molecules for PPC proliferation may contribute to the development of cell therapy for T1D using a regenerative medicine approach.

Keywords

diabetes, induced pluripotent stem cell, pancreatic progenitor cell, small molecule, proliferation

1. Introduction

β cell replacement treatment for type 1 diabetes (T1D) requires a vast number of islet cells that nears the order of billions (Shapiro et al., 2006). Donor tissues are the most common source of these cells, but are scarce, which has encouraged research in alternative sources such as human pluripotent stem cells. Many groups including ours have reported protocols that induce the differentiation of human embryonic stem cells (hESCs) or induced pluripotent stem cells (hiPSCs) into pancreatic β-like cells by utilizing guided differentiation *in vitro* with or without *in vivo* maturation (D'Amour et al., 2006; Kroon et al., 2008; Pagliuca et al., 2014; Rezania et al., 2014; Russ et al., 2015; Toyoda et al., 2015). The feasibility of hESC/iPSC-derived pancreatic cells for diabetes treatment is well demonstrated by the curative effects of these cells implanted in diabetic animal models (Kroon et al., 2008; Rezania et al., 2012).

Despite the success in hESC/iPSC-derived pancreatic cell generation, a practical challenge still remains in cell preparation for the establishment of cell therapy in clinical setting. Specifically, protocols that differentiate pluripotent stem cells to pancreatic lineage at high efficiency and numbers are required. Recent reports have shown the establishment of a scalable system to generate hESC/iPSC-derived pancreatic cells (Pagliuca et al., 2014; Schulz et al., 2012). In this system, an initial step requires the massive propagation of undifferentiated stem cells as the starting cell source. Although this system fits the original advantageous concept of generating hESC/iPSC-derived pancreatic cells, the maintenance of such a large scale of undifferentiated cells at the pluripotent state can be cumbersome. Further, undesired cell types that arise from inefficient differentiation at each step affect the cell quality. In view of the cost, preparation time, management and quality of the generated cells, a more fine-tunable system is preferred for clinical applications.

Pancreas development begins at around mouse embryonic day (E) 9.5 when pancreatic progenitor cells (PPCs) expressing the transcription factor pancreatic and duodenal homeobox 1 (Pdx1) develop into pancreatic buds (Jørgensen et al., 2007). Lineage tracing studies have indicated that $Pdx1^+$ PPCs are required for pancreas development, as they give rise to all cell types found in the pancreas (Gu et al., 2003). Therefore, the amplification of *in vitro*-generated PPCs would be advantageous, as it shortens the handling period for cells in large-scale culture. A number of small molecules have been identified as proliferation inducers for several cell types including mouse satellite cells, mouse and human retinal pigment epithelial cells, and human adult β cells (Billin et al., 2016; Shen et al., 2013; Swoboda et al., 2013; Wang et al., 2015). However, knowledge of the PPC proliferation mechanism is currently limited, and proliferation inducers for stem cell-derived PPCs have not been well investigated.

The purpose of the current study was to screen and identify small molecules that

promote the proliferation of hiPSC-derived PPCs. We identified one promising compound, AT7867, which underscores the applicability of an efficient production system for stem cell-derived pancreatic cells. The use of small molecules for PPC proliferation may aid in generating the large numbers of cells required for implantation and *in vitro* studies.

2. Materials and Methods

2.1. hiPSC/ESC culture and pancreatic differentiation.

Experiments with iPSCs were approved by the ethics committee of the Department of Medicine and Graduate School of Medicine, Kyoto University. Two hiPSC lines, 585A1 (Okita et al., 2013) and Ff-I01, and one hESC line, KhES-3 (Suemori et al., 2006), were maintained and passaged in Essential 8 medium (Thermo Fisher Scientific) or StemFit AK02N/03N (Reprocell). Cells were directed to differentiate through key stages of pancreatic differentiation (Stage 1: SRY (sex determining region Y)-box 17 (SOX17)-expressing definitive endoderm cells (DECs), Stage 2: hepatocyte nuclear factor 4α (HNF4α)-expressing primitive gut tube cells (PGTCs), and Stage 3: PDX1-expressing PPCs), as described previously with modifications (Toyoda et al., 2015).

2.2. Small molecule screening.

To prepare cells for screening, Stage 3 day 2 cells were dissociated and seeded on Matrigel (BD Biosciences)-coated plates at 1.2×10^5 cells/cm^2. Twenty-four hours after cell seeding, cells were fed with Improved MEM (iMEM; Thermo Fisher Scientific) supplemented with 0.5× B27 (Thermo Fisher Scientific), 100 U/ml Penicillin-Streptomycin (P/S; Thermo Fisher Scientific), 100 ng/ml keratinocyte growth factor (KGF; R&D Systems), 0.2 μM LDN193189 (LDN; Axon Medchem) and 50 ng/ml epidermal growth factor (EGF; R&D Systems) to maintain the pancreatic lineage cells (Schulz et al., 2012). A custom-prepared small molecule library composed of kinase inhibitors was supplied in arrayed format in 384-well plates and 1 mM stocks in dimethyl sulfoxide (DMSO). Individual compounds were diluted in two steps in two separate plates and transferred into assay plates by using Biomek NX (Beckman Coulter) at the final concentration of 1 μM. After four days of treatment, plates were assayed for cell number as determined by Hoechst 33342 (Thermo Fisher Scientific) staining. The quantification method is described in Supplemental methods. Each assay plate was designed to contain DMSO control wells whose mean cell count was used to normalize each plate.

2.3. Vascular endothelial cell and pancreatic endocrine cell differentiation.

hiPSCs were differentiated into vascular endothelial cells (VECs) as described previously (Tatsumi et al., 2011). Briefly, undifferentiated hiPSCs were fed with 5 μM BIO (SIGMA) for three days followed by incubation with vascular endothelial growth factor (TOMBO Biosciences) for four days. On day 7, cells expressing fetal liver kinase 1 (FLK1) and vascular endothelial cadherin (VE-cadherin) were sorted using flow cytometry and replated on gelatin-coated plates at 3.1×10^4 cells/cm^2 in Endothelial Basal Medium-2 (Lonza) for two days before the addition of the compound.

Differentiation into insulin-producing endocrine cells (ECs) was performed as follows. PPCs before or after cell proliferation by the compound were dissociated and made into aggregates on a low-binding plate (Greiner). Cells were fed with medium containing iMEM supplemented with 0.5× B27, 100 U/ml P/S and factors known to induce endocrine differentiation including 10 μM Alk 5 inhibitor II (Wako), 1 μM Triiodothyronine (T3; Merck Millipore), 0.1 μM LDN and 1 μM γ-secretase inhibitor XXI (Merck Millipore) for 12 days (Mfopou et al., 2010; Pagliuca et al., 2014; Rezania et al., 2014).

2.4. Statistical analysis.

All statistical tests were performed by Prism 7.0 (GraphPad) using Student's *t*-test for the statistical significance in mean values of two-sample comparison, one-way ANOVA with a Dunnett test for comparisons with control treatment, and two-way ANOVA with a Bonferroni test, one-way ANOVA or two-way repeated measures ANOVA with a Tukey test for multiple comparisons between treatments. $P < 0.05$ was considered statistically significant for all analyses.

3. Results

3.1. Small molecule screening with hiPSC-derived PPCs.

The screen was designed to identify small molecules that promote the proliferation of $PDX1^+$ PPCs. Uniform induction into PPCs was routinely achieved with >90% efficiency at day 11, and the proportion of $PDX1^+$ cells was not affected by replating (Figures 1A, S1A and B).

Next, we developed an automated 96-well based chemical screening platform that outputs total cell numbers from each well. We defined hit compounds as those that scored at least a two-fold increase in cell number compared with DMSO control. Of the 1,327 small molecules tested, three compounds, AT7867, SB525334 and dasatinib, satisfied our criterion and were designated as primary hit compounds (Figures 1B and C). After a dose-response test of the three compounds, AT7867 was identified as the most effective small molecule and was investigated further (Figures 1D, E and S1C). AT7867 treatment significantly increased the cell number at a relatively low concentration range (0.05 – 1 μM), while higher concentration treatments were detrimental to the cells. Notably, while control-treated cells remained low in PDX1 staining intensity after four days of treatment, AT7867-treated cells showed relatively stronger intensity, suggesting maintenance of the pancreatic progenitor cell state (Figure 1F).

3.2. AT7867 is a proliferation-promoting factor rather than an apoptosis suppressor.

The effect of AT7867 treatment on the increased cell number was first observed at day 2 of treatment, and plateaued at around day 6 when the $PDX1^+$ cell number increased by approximately five-fold (Figure 2A). Of note, the AT7867-treated cells maintained a high proportion of $PDX1^+$ cells (>95%), whereas the control cells had a lower percentage (~60%) over the course of the experiment (Figures 2B and C). Immunostaining with a cell proliferation marker, Ki67, revealed that PDX1 and Ki67 were co-expressed in AT7867-treated cells at a higher proportion for longer time (over six days) than in control-treated cells (Figures 2B and D). $PDX1^-Ki67^+$ cells were rarely found in control or AT7867-treated cells, further suggesting that AT7867 may have the potential to maintain cell proliferation activity only in PPCs (Figure S2A). Moreover, the effect of AT7867 treatment was tested on two other hESC/iPSC lines (see Materials and Methods). AT7867 also induced the proliferation of PPCs differentiated from these cell lines, which suggests versatility of the small molecule (Figure S2B and C).

The acceleration of cell proliferation by adding small molecules or the overexpression of cell cycle activators has been reported to induce cell cycle arrest and DNA damage (Rieck et al., 2012; Rodriguez et al., 2012). Phospho-histone H3 (pHH3) and phospho-histone H2AX (pHH2AX) are useful markers for identifying cells in mitotic phase and cells with DNA damage, respectively (Kleiner et al., 2015; Tessem et al., 2014). AT7867

treatment induced and maintained a relatively higher proportion of $pHH3^+$ cells, suggesting that AT7867-treated cells proliferate through complete activation of the cell cycle (Figure 2E). Consistent with a previous report (Zhang et al., 2015), approximately 10% of undifferentiated iPSCs were stained with pHH2AX antibody, while only a small proportion of cells were $pHH2AX^+$ in AT7867-treated cells, confirming no increased DNA damage (Figures 2F and S2D). Furthermore, AT7867 treatment neither enhanced nor suppressed the proportion of cleaved-caspase 3^+ cells, suggesting that the increase in $PDX1^+$ PPCs is brought about by AT7867 having a proliferation-promoting effect rather than an apoptosis suppressing effect (Figure 2G). Taken altogether, AT7867 treatment potentiates PPCs' proliferative capacity through activation of the cell cycle without affecting genome DNA or cell death signaling.

3.3. PPCs are specifically proliferated by AT7867 treatment.

To investigate whether AT7867 can promote the proliferation of other cell types at three distinct pancreatic differentiation stages, we analyzed cell numbers after AT7867 treatment in DECs, PGTCs and PPCs (Figure 1A). $SOX17^+$ DECs gradually decreased in number and proportion in both control and AT7867 treatment groups (Figure 3A). Although we observed the maintenance of the proportion of $HNF4\alpha^+$ PGTCs, AT7867 treatment did not increase the number (Figure 3B). $PDX1^+$ cells were induced from PGTCs with AT7867 treatment, but the $PDX1^+$ cell number did not significantly differ from control DMSO treatment, suggesting that AT7867 does not induce differentiation to PPCs (Figure S3). On the contrary to these cell types, AT7867 treatment significantly increased only the $PDX1^+$ PPC number (Figure 3C). As expected, we observed no increase in $PDX1^-$ cell number (data not shown).

To further examine the cell type dependency of AT7867 on cellular proliferation other than endodermal lineage cells, we investigated the effect of AT7867 on hiPSC-derived vascular endothelial cells (VECs), a mesoderm lineage cell type. A comparison of cell numbers showed no significant difference between control and AT7867 groups (Figure 3D). Together, the effect of AT7867 to promote cellular proliferation is specific to $PDX1^+$ PPCs, at least among the cell types tested here.

3.4. Inhibition of AKT/p70S6K/RSK is not the mechanism of PPC proliferation.

We aimed to identify the direct molecular target of AT7867 that is responsible for the cellular proliferation. AT7867 is known to strongly block AKT phosphorylation (IC_{50} of 32/17/47 nM for AKT1/2/3, respectively) and also inhibit several other kinases including p70S6K and RSK at greater IC_{50} values (Grimshaw et al., 2010). More selective inhibitors of these kinases (GDC-0068, AZD5363, MK-2206, BI-D1870 and PF-4708671) did not increase the number of PPCs (Figure S4). We therefore leave the identification of target molecules of AT7867 for future studies.

3.5. AT7867-treated cells differentiate into pancreatic endoderm and subsequently endocrine cells in vitro.

During mouse pancreas development, $PDX1^+$ foregut epithelium (an *in vivo* counterpart of PPCs) evaginates to form pancreatic buds on the dorsal and ventral sides, and the earliest pancreas-committed cells (pancreatic endodermal cells) are marked by the expression of three key genes, *Pdx1, NK6 homeobox 1* (*Nkx6.1*) and *pancreas transcription factor, 1a* (*Ptf1a*) (Hald et al., 2008; Jørgensen et al., 2007). Our previous report showed that cell density is one key factor that contributes to pancreatic differentiation and that increased cell density and a combination of soluble factors interdependently signal cells to further differentiate (Toyoda et al., 2015). These findings imply that the cell number increase by AT7867 treatment and the combination of soluble factors might trigger the upregulation of these genes. In fact, *NKX6.1* and *PTF1A* were upregulated at the mRNA level in AT7867-treated cells initially seeded at a density of 1.2×10^5 cells/cm^2 and cultured in Stage 4 (S4) medium containing KGF, LDN and EGF (Figure 4A). Flow cytometry analysis showed that 48.4 ± 7.8% of total cells co-expressed PDX1 and NKX6.1 at the protein level after 4-day culture with AT7867 in S4 medium (Figures 4B, S5A and B). To further investigate whether AT7867 directly induces $NKX6.1^+$ cells, AT7867 treatment at various initial cell densities or with different culture media were considered. Although AT7867 treatment increased PPC number at all seeding densities, cells co-expressing PDX1 and NKX6.1 were observed when the PPCs were seeded above a certain cell density (Figures S5C and D). Moreover, cell proliferation with AT7867 in Stage 3 (S3) medium was not sufficient to induce $NKX6.1^+$ cells (Figure S5E). These results suggest that PPCs that proliferated upon AT7867 treatment can differentiate into pancreatic endoderm cells and that AT7867 works for pancreatic endoderm differentiation in an orchestrated manner with the soluble factors rather than in a direct manner.

To examine whether PPCs proliferated by the AT7867 treatment differentiate into pancreatic ECs, PPCs were further induced to differentiate into ECs before or after AT7867 treatment (Figure 4C). We found that AT7867 treatment with either S3 or S4 medium resulted in a higher proportion of C-$peptide^+$ cells compared to PPCs that did not receive the treatment (Figures 4D, E and F). This difference could be due to the fact that AT7867 treatment changes the cellular state of PPCs in a preferable way for EC commitment. Further analysis revealed that approximately half of C-$peptide^+$ cells were GLUCAGON-negative before and after AT7867 treatment. Collectively, these data suggest that AT7867 is a potent proliferation-promoting factor for $PDX1^+$ PPCs, which retain the ability to further differentiate into ECs including β-like cells *in vitro*.

4. Discussion

For the use of *in vitro*-generated cells to treat human diseases such as T1D, a large number of therapeutically useful cells at high purity are needed. The chemical screening approach used here shows that it is feasible to identify factors that potentially fulfill this requirement. In this study, we identified one small molecule, AT7867, that promotes the efficient proliferation of PPCs derived from hiPSCs in two-dimensional culture. PPCs treated with AT7867 maintained a high proportion of cells expressing PDX1 that possessed enhanced differentiation potential into pancreatic ECs. In addition, the AT7867-treated PPCs did not show an increased proportion of cells with DNA damage, which affirms the benefits of a small molecule strategy for the *in vitro* generation of stem cell-derived pancreatic cells.

The development of scalable hESC/iPSC-derived pancreatic cell generation also holds great value for drug screening and toxicity tests for diabetes. However, more cost-effective, well-controlled systems are desired in the cell preparation process that goes beyond the amplification of undifferentiated hESCs/iPSCs (Pagliuca et al., 2014; Schulz et al., 2012). The proliferation of PPCs based on the use of small molecules may provide such cost-effective and fine-tunable systems. Moreover, several chemical screening studies showed the identification of proliferation inducers for human adult β cells (Shen et al., 2013; Wang et al., 2015). Whether the proliferation of PPCs could be further improved by the combinatorial treatment with these compounds should be explored in future studies.

It was reported that co-culture systems with organ-matched mesenchymal cell lines secreting unknown factors support the self-renewal of hESC-derived definitive endoderm and pancreatic endocrine progenitor cell populations (Sneddon et al., 2012). Nevertheless, variability of the supporting cells between passages affects the proliferation and differentiation outcomes, which limits the use of these systems. In addition, co-culture systems potentially suffer from contamination unless well-established measures for the elimination of the supporting cells are implemented. Small molecules, on the other hand, have great promise to serve as substitutes and may enable the establishment of efficient and stable protocols. Our data showed that AT7867 treatment increased the cell number in a cell type-dependent manner, specifically increasing the number of PPCs. Therefore, precise cell amplification can be achieved in the pancreatic cell preparation process by using small molecules without any need for other cell sources.

The possibility that AT7867 may be a direct NKX6.1 inducer still remains, but our results suggest that the induction into $PDX1^{+}NKX6.1^{+}$ cells was triggered at least partly by the combination of increased cell density and soluble factors. In fact, we were able to observe $PDX1^{+}NKX6.1^{+}$ cells only in dense areas where proliferated PPCs made more contact with neighboring cells, an observation consistent with our previous report (Toyoda et al., 2015).

Although several groups have reported the biological activities of AT7867, our

results indicated somewhat contradictory cellular responses to its known function (Grimshaw et al., 2010). The inhibition of PI3K/AKT by specific inhibitors including AT7867 results in the downregulation of downstream phosphorylation signaling in tumorigenic cell lines, causing a reduction in tumor size in *in vivo* mouse models (Grimshaw et al., 2010; Zhang et al., 2016). Here, we unexpectedly observed that AT7867 increased the number of PPCs, but the mechanism of action remains unrevealed since other selective AKT inhibitors did not show similar effects. This result indicates that there are either specific biological targets of AT7867 besides AKT or distinctive modulatory functions of the signaling axis on PPC proliferation. Further mechanistic elucidation of the signaling pathways will provide novel insights into PPC proliferation and endocrine cell commitment and may clarify early pancreas development.

To conclude, our study proposes a novel small molecule-based proliferation of PPCs for use in regenerative medicine and *in vitro* studies.

Acknowledgments

This work was supported in part by funding from the Takeda Science Foundation to T.T., the Suzuken Memorial Foundation to T.T., Mitsui Life Social Welfare Foundation to K.O., the Life Science Foundation of Japan to K.O., Japan Diabetes Foundation to K.O., Grant-in-Aid for JSPS Research Fellows (JSPS KAKENHI Grant Number 17J07622) to A.K. and Scientific Research (C) (JSPS KAKENHI Grant Number 15K09385) to T.T., and the Japan Agency for Medical Research and Development (AMED) through its research grant "Core Center for iPS Cell Research, Research Center Network for Realization of Regenerative Medicine" to K.O. A.K. was supported by a fellowship from JSPS. The authors thank Dr. Kanae Mitsunaga for her technical assistance in the flow cytometry analysis and Dr. Peter Karagiannis for reading the manuscript.

References

Billin, A.N., Bantscheff, M., Drewes, G., et al., 2016. Discovery of novel small molecules that activate satellite cell proliferation and enhance repair of damaged muscle. ACS Chem. Biol. 11 (2), 518–529.

D'Amour, K. a, Bang, A.G., Eliazer, S., et al., 2006. Production of pancreatic hormone-expressing endocrine cells from human embryonic stem cells. Nat. Biotechnol. 24 (11), 1392–401.

Grimshaw, K.M., Hunter, L.-J.K., Yap, T. a, et al., 2010. AT7867 is a potent and oral inhibitor of AKT and p70 S6 kinase that induces pharmacodynamic changes and inhibits human tumor xenograft growth. Mol. Cancer Ther. 9 (5), 1100–10.

Gu, G., Brown, J.R., Melton, D.A., 2003. Direct lineage tracing reveals the ontogeny of pancreatic cell fates during mouse embryogenesis. Mech. Dev. 120 (1), 35–43.

Hald, J., Sprinkel, A.E., Ray, M., et al., 2008. Generation and characterization of Ptf1a antiserum and localization of Ptf1a in relation to Nkx6.1 and Pdx1 during the earliest stages of mouse pancreas development. J. Histochem. Cytochem. 56 (6), 587–95.

Jørgensen, M.C., Ahnfelt-Rønne, J., Hald, J., et al., 2007. An illustrated review of early pancreas development in the mouse. Endocr. Rev. 28 (6), 685–705.

Kleiner, R.E., Verma, P., Molloy, K.R., et al., 2015. Chemical proteomics reveals a γH2AX-53BP1 interaction in the DNA damage response. Nat. Chem. Biol. 11 (10), 807–814.

Kroon, E., Martinson, L.A., Kadoya, K., et al., 2008. Pancreatic endoderm derived from human embryonic stem cells generates glucose-responsive insulin-secreting cells in vivo. Nat Biotechnol 26 (4), 443–452.

Mfopou, J.K., Chen, B., Mateizel, I., et al., 2010. Noggin, retinoids, and fibroblast growth factor regulate hepatic or pancreatic fate of human embryonic stem cells. Gastroenterology 138 (7), 2233–45, 2245–14.

Okita, K., Yamakawa, T., Matsumura, Y., et al., 2013. An efficient nonviral method to generate integration-free human-induced pluripotent stem cells from cord blood and peripheral blood cells. Stem Cells 31 (3), 458–466.

Pagliuca, F.W., Millman, J.R., Gürtler, M., et al., 2014. Generation of functional human pancreatic β cells in vitro. Cell 159 (2), 428–439.

Rezania, A., Bruin, J.E., Arora, P., et al., 2014. Reversal of diabetes with insulin-producing cells derived in vitro from human pluripotent stem cells. Nat Biotechnol 32 (11), 1121–1133.

Rezania, A., Bruin, J.E., Riedel, M.J., et al., 2012. Maturation of human embryonic stem cell-derived pancreatic progenitors into functional islets capable of treating pre-existing diabetes in mice. Diabetes 61 (8), 2016–2029.

Rieck, S., Zhang, J., Li, Z., et al., 2012. Overexpression of hepatocyte nuclear factor-4α initiates cell cycle entry, but is not sufficient to promote β-cell expansion in human islets. Mol. Endocrinol. 26 (September), 1590–602.

Rodriguez, R., Miller, K.M., Forment, J. V, et al., 2012. Small-molecule-induced DNA damage identifies alternative DNA structures in human genes. Nat Chem Biol 8 (3), 301–310.

Russ, H. a, Parent, A. V, Ringler, J.J., et al., 2015. Controlled induction of human pancreatic progenitors produces functional beta-like cells in vitro. EMBO J. 34 (13), e201591058.

Schulz, T.C., Young, H.Y., Agulnick, A.D., et al., 2012. A scalable system for production of functional pancreatic progenitors from human embryonic stem cells. PLoS One 7 (5), e37004.

Shapiro, M.J., Ricordi, C., Hering, B.J., et al., 2006. International trial of the Edmonton protocol for islet transplantation. N. Engl. J. Med. 355 (13), 1318–30.

Shen, W., Tremblay, M.S., Deshmukh, V.A., et al., 2013. Small-molecule inducer of β cell proliferation identified by high-throughput screening. J. Am. Chem. Soc. 135 (5), 1669–1672.

Sneddon, J.B., Borowiak, M., Melton, D.A., 2012. Self-renewal of embryonic-stem-cell-derived progenitors by organ-matched mesenchyme. Nature 491 (7426), 765–768.

Suemori, H., Yasuchika, K., Hasegawa, K., et al., 2006. Efficient establishment of human embryonic stem cell lines and long-term maintenance with stable karyotype by enzymatic bulk passage. Biochem. Biophys. Res. Commun. 345, 926–932.

Swoboda, J.G., Elliott, J., Deshmukh, V., et al., 2013. Small molecule mediated proliferation of primary retinal pigment epithelial cells. ACS Chem. Biol. 8 (7), 1407–1411.

Tatsumi, R., Suzuki, Y., Sumi, T., et al., 2011. Simple and highly efficient method for production of endothelial cells from human embryonic stem cells. Cell Transplant. 20 (9), 1423–1430.

Tessem, J.S., Moss, L.G., Chao, L.C., et al., 2014. Nkx6.1 regulates islet β-cell proliferation via Nr4a1 and Nr4a3 nuclear receptors. Proc. Natl. Acad. Sci. U. S. A. 111 (14), 5242–7.

Toyoda, T., Mae, S.I., Tanaka, H., et al., 2015. Cell aggregation optimizes the differentiation of human ESCs and iPSCs into pancreatic bud-like progenitor cells. Stem Cell Res. 14 (2), 185–197.

Wang, P., Alvarez-Perez, J.-C., Felsenfeld, D.P., et al., 2015. A high-throughput chemical screen reveals that harmine-mediated inhibition of DYRK1A increases human pancreatic beta cell replication. Nat. Med. 21 (4), 383–388.

Zhang, Q., Yan, H., Wang, J., et al., 2016. Chromatin remodeling gene AT-rich interactive domain-containing protein 1A suppresses gastric cancer cell proliferation by targeting PIK3CA and PDK1. Oncotarget 7 (29), 1–15.

Zhang, W., Li, J., Suzuki, K., et al., 2015. A Werner syndrome stem cell model unveils heterochromatin alterations as a driver of human aging. Science 348 (6239), 1160–1163.

Figure legends

Figure 1. Small molecule screen identifies AT7867 as a proliferation-promoting factor for PDX1$^+$ pancreatic progenitor cells.

(A) Directed differentiation from hiPSCs to pancreatic lineage and scheme of small molecule screen.

(B) Results of small molecule screen showing the normalized cell number to DMSO control. Images were captured, and the number of stained nuclei was quantified by the image analyzer.

(C) Representative images of nuclear staining for the hit compounds.

(D) Chemical structure of AT7867.

(E) Dose response of AT7867 on the number of hiPSC-derived PPCs.

(F) Representative images of cells treated with AT7867 for four days and stained with PDX1 antibody from three independent experiments.

iPSC, induced pluripotent stem cell; DEC, definitive endoderm cell; PGTC, primitive gut tube cell; PPC, pancreatic progenitor cell. Data are presented as the mean ± s.d. from three independent experiments in (E**)**. *P < 0.05, **P < 0.01, one-way ANOVA with a Dunnett test for multiple comparisons versus 0 μM in (E). Scale bars, 100 μm.

Figure 2. AT7867 treatment maintains PDX1$^+$ pancreatic progenitor cells in proliferative state.

(A) Quantitative analysis of PPC number by the image analyzer. PPCs were treated with AT7867 in the presence of KGF, LDN and EGF for eight days. DMSO was used as a control.

(B) Representative images of Ki67 staining at day 4 from three independent experiments.

(C, D) The proportions of PDX1$^+$ (C) and PDX1$^+$Ki67$^+$ cells (D) during the eight-day culture evaluated by the image analyzer.

(E-G) Cells were stained with the following antibodies: pHH3 for cells in M phase of cell division, pHH2AX for cells with DNA damage, and cleaved caspase-3 (CC3) for cells undergoing apoptosis.

Black circles denote cells treated with AT7867, and white circles denote DMSO control. Data are presented as the mean ± s.d. from three independent experiments in (A), (C)-(G). *P < 0.05, **P < 0.01, ***P < 0.001, two-way ANOVA with a Bonferroni test for multiple comparisons between treatments at each time point in (A) and two-way repeated measures ANOVA with a Tukey test in (C-G). Scale bar, 100 μm.

Figure 3. AT7867 treatment specifically increases the number of PDX1$^+$ cells.

(A-C) Quantitative analysis of the proportions and numbers of SOX17$^+$ DECs (A), HNF4α$^+$ PGTCs (B) and PDX1$^+$ PPCs (C) by the image analyzer. Cells were replated one day prior to the end of differentiation Stage 1, 2 or 3. On the following day, cells were cultured in basal

medium containing stage specific differentiation factors with AT7867 or DMSO. Representative images are shown of cells on day 0 (before treatment) and day 4 (after four days of AT7867 or DMSO treatment) from three independent experiments.
(D) Quantitative analysis of vascular endothelial cell (VEC) number after four days of AT7867 or DMSO treatment.
Black circles denote cells treated with AT7867, and white circles denote DMSO control. Data are presented as the mean ± s.d. from three independent experiments. ***$P < 0.001$, n.s., not significant, two-way repeated measures ANOVA with a Tukey test in (A-C), and paired Student's two-tailed *t*-test in (D). Scale bars, 50 μm.

Figure 4. AT7867-treated cells differentiate into pancreatic endoderm and insulin-producing cells.
(A) Gene expression of AT7867-treated cells for *PDX1*, *PTF1A* and *NKX6.1*.
(B) The proportion of $PDX1^{+}NKX6.1^{+}$ cells analyzed by flow cytometry.
(C) Scheme of the EC differentiation. All cells were treated with EC differentiation cues for the same duration before or after 4-day AT7867 treatment.
(D) Representative images of C-$peptide^{+}$ ECs co-stained with PDX1 and GLUCAGON from three independent experiments.
(E) Representative flow cytometry plots showing co-expression of PDX1 and C-peptide.
(F) Flow cytometry quantification of C-$peptide^{+}$ cells and co-expression of PDX1 and GLUCAGON.
Data are presented as the mean ± s.d. from three independent experiments in (A), (B) and (F). *$P < 0.05$, **$P < 0.01$, paired Student's two-tailed *t*-test in (B) and one-way ANOVA with a Tukey test in (F). Scale bar, 100 μm.

Figure 1

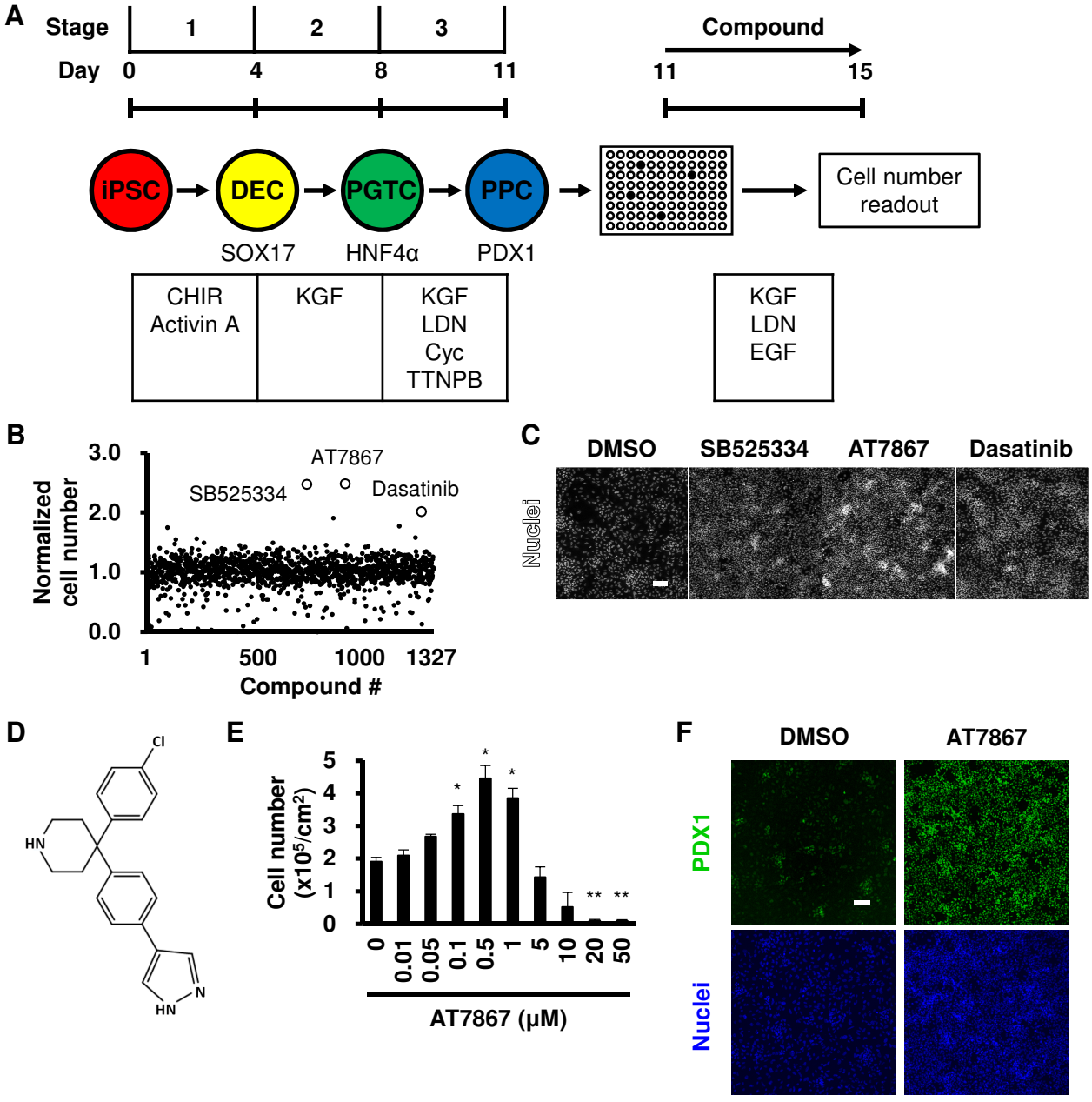
A
Stage
1
2
3
Day
0
4
8
11
Compound
11
15
iPSC
DEC
PGTC
PPC
Cell number readout
SOX17
HNF4α
PDX1
CHIR
Activin A
KGF
KGF
LDN
Cyc
TTNPB
KGF
LDN
EGF
B
Normalized cell number
3.0
2.0
1.0
0.0
AT7867
SB525334
Dasatinib
1
500
1000
1327
Compound #
C
DMSO
SB525334
AT7867
Dasatinib
Nuclei
D
Cl
HN
HN
N
E
Cell number (x10⁵/cm²)
5
4
3
2
1
0
*
*
*
**
**
0
0.01
0.05
0.1
0.5
1
5
10
20
50
AT7867 (μM)
F
DMSO
AT7867
PDX1
Nuclei

Figure 2

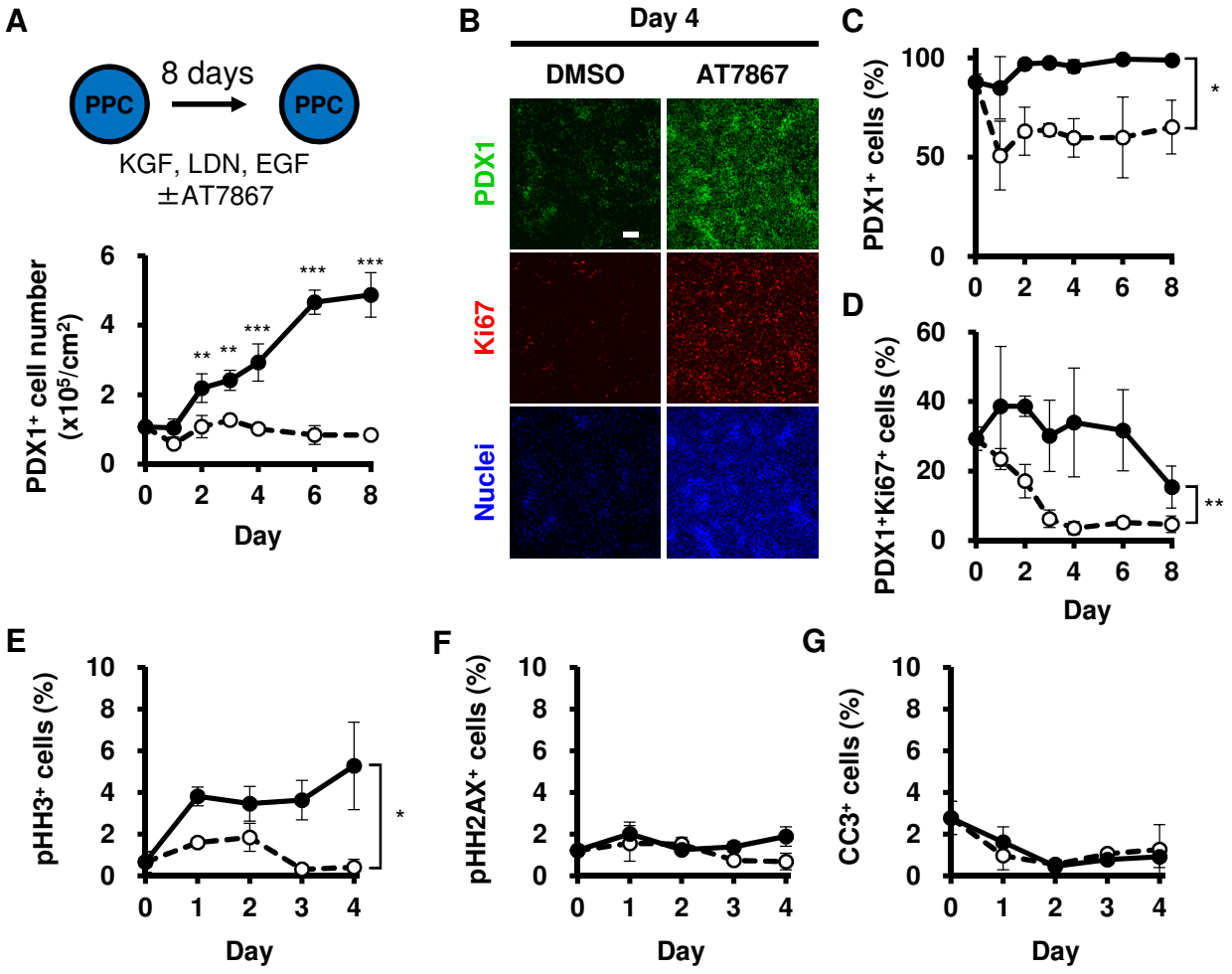
A
PPC
8 days
PPC
KGF, LDN, EGF
±AT7867
PDX1⁺ cell number (x10⁵/cm²)
Day
B
Day 4
DMSO
AT7867
PDX1
Ki67
Nuclei
C
PDX1⁺ cells (%)
D
PDX1⁺Ki67⁺ cells (%)
Day
E
pHH3⁺ cells (%)
Day
F
pHH2AX⁺ cells (%)
Day
G
CC3⁺ cells (%)
Day

Figure 3

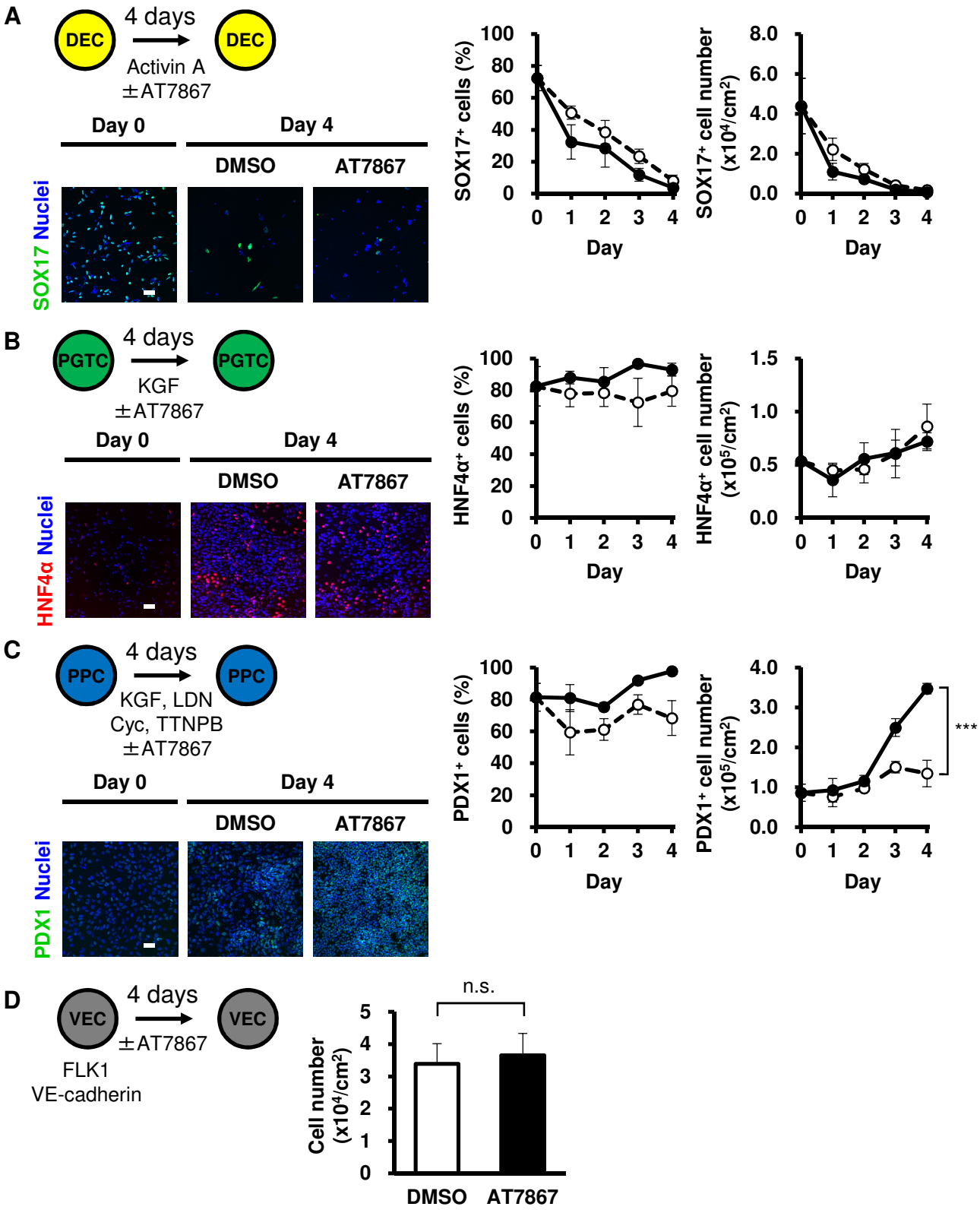
A
DEC
4 days
DEC
Activin A
±AT7867
Day 0
Day 4
DMSO
AT7867
SOX17 Nuclei
SOX17⁺ cells (%)
SOX17⁺ cell number (x10⁴/cm²)
Day
B
PGTC
4 days
PGTC
KGF
±AT7867
HNF4α Nuclei
HNF4α⁺ cells (%)
HNF4α⁺ cell number (x10⁵/cm²)
C
PPC
4 days
PPC
KGF, LDN
Cyc, TTNPB
±AT7867
PDX1 Nuclei
PDX1⁺ cells (%)
PDX1⁺ cell number (x10⁵/cm²)
***
D
VEC
4 days
VEC
±AT7867
FLK1
VE-cadherin
n.s.
Cell number (x10⁴/cm²)

Figure 4

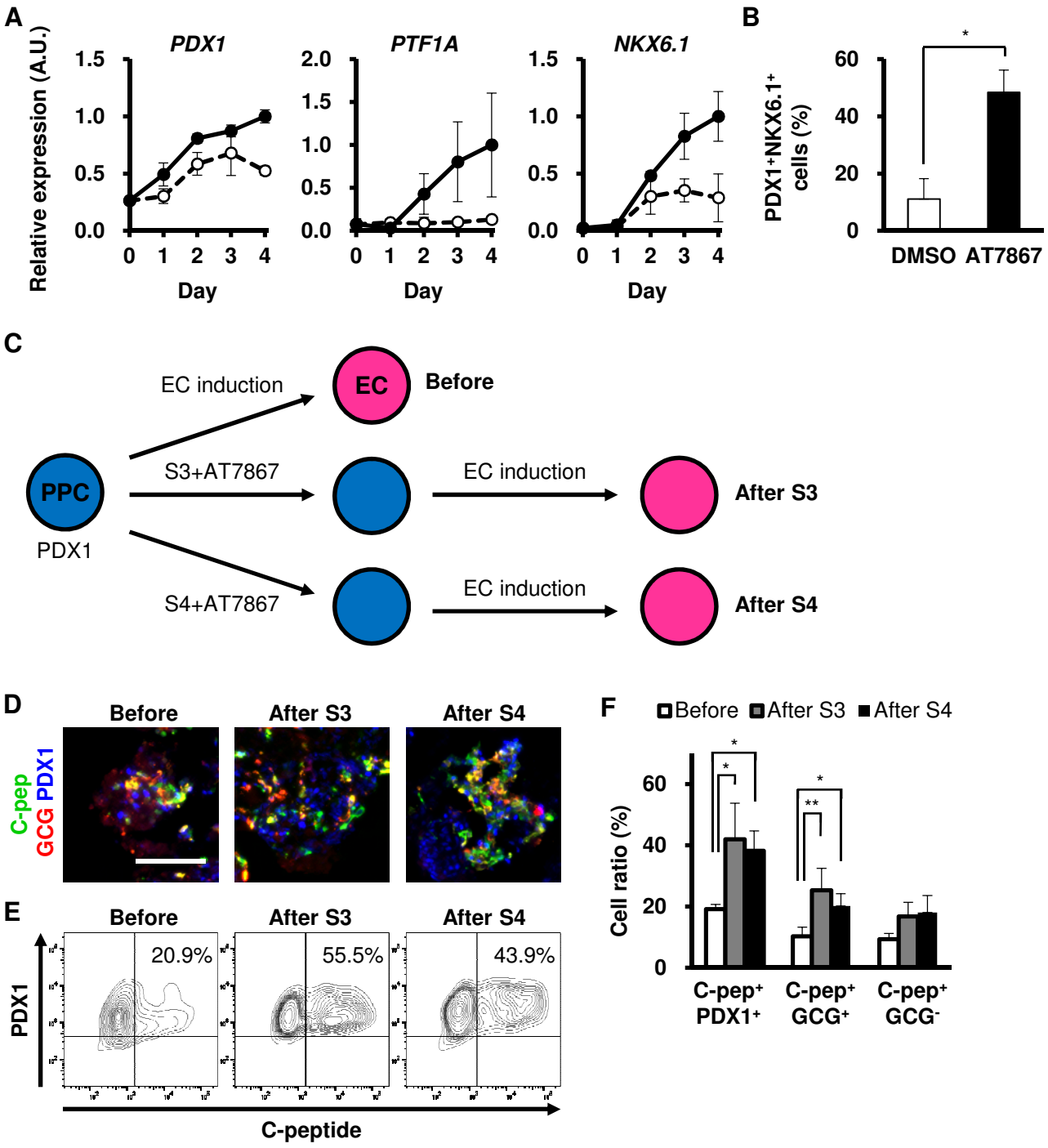
A
PDX1
PTF1A
NKX6.1
Relative expression (A.U.)
Day
B
PDX1+NKX6.1+ cells (%)
DMSO
AT7867
C
EC induction
EC
Before
PPC
PDX1
S3+AT7867
EC induction
After S3
S4+AT7867
EC induction
After S4
D
Before
After S3
After S4
C-pep
GCG
PDX1
E
Before
After S3
After S4
20.9%
55.5%
43.9%
PDX1
C-peptide
F
Before
After S3
After S4
Cell ratio (%)
C-pep+ PDX1+
C-pep+ GCG+
C-pep+ GCG-

Supplemental methods

Immunofluorescence staining.

Cells were gently washed with phosphate-buffered saline (PBS) and fixed with 4% paraformaldehyde for 20 minutes at 4°C. The fixed cells were washed twice with PBS and blocked with blocking solution containing 5% donkey serum in 0.4% Triton X-100 for 30 minutes at room temperature. The cells were incubated with the primary antibodies listed in Supplemental Table 1 overnight at 4°C in blocking solution. The primary antibodies were visualized using secondary antibodies conjugated with AlexaFluor-488, -546 or -647 (Thermo Fisher Scientific).

Imaging and quantification.

Stained cells were imaged using a fluorescence microscope BZ-9000 (Keyence). For quantification, a CellInsight™ NXT or ArrayScan™ VTI automated screening platform (Thermo Fisher Scientific) was used, and cell counts and signal intensities were measured and analyzed using HCS Studio™ 2.0 Cell Analysis Software (Thermo Fisher Scientific). The system was programmed to capture and analyze at least three images per well for chemical screening or nine images per well for other experiments.

Flow cytometry.

Differentiated cells were dissociated and fixed with Cytofix/Cytoperm Kit (BD Biosciences) according to the manufacturer's protocol. Stained cells were analyzed with the FACSAria™ II flow cytometer (BD Biosciences), and plots were processed using FACSDiva (BD Biosciences) and FlowJo (Tree Star Inc).

Quantitative polymerase chain reaction (qPCR).

RNA was isolated from cells using RNeasy kit (Qiagen), and reverse transcription was performed with ReverTra Ace qPCR RT Master Mix (Toyobo) and oligo (dT)20 primer. Quantitative PCR was carried out using SYBR Premix Ex Taq II (Takara) on a StepOnePlus™ Real-Time PCR System (Applied Biosystems). The list of primer sequences used is provided in Supplemental Table 2. Relative fold changes in the gene expression were calculated using the relative standard curve method. Gene expression was normalized to GAPDH expression level.

Supplemental figure legends

Figure S1. The effects of replating cells and two other hit compounds. (A) The effect of replating PPCs on PDX1 expression evaluated by immunofluorescence staining. Scale bar, 100 μm. (B) Flow cytometric analysis of PDX1 protein expression in undifferentiated iPSCs and PPCs with or without replating. Over 90% of differentiated cells express PDX1. (C) Dose response of two other hit compounds on the number of PPCs (n = 1).

Figure S2. The adverse effect of AT7867 treatment is minimal. (A) The effect of AT7867 on the proportion of $PDX1^{-}Ki67^{+}$ cells analyzed by the image analyzer. AT7867 treatment does not promote the proliferation of $PDX1^{-}$ cells. DMSO (white), AT7867 (black). (B) Representative images of PPCs treated with AT7867 at day 4 in two other pluripotent stem cell lines, KhES-3 and Ff-I01, with the nuclei indicated in blue. (C) Quantitative analysis of PPC number and the proportions of $PDX1^{+}$ and $PDX1^{+}Ki67^{+}$ cells in KhES-3 (left) and Ff-I01 (right) cell lines. DMSO (white), AT7867 (black). (D) Immunofluorescence staining for a DNA damage marker, pHH2AX. The proportion of pHH2AX-stained cells after 4 days of AT7867 or DMSO treatment was not increased as compared to hiPSCs or day 0 cells. Representative images of three independent experiments are shown. Data are presented as the mean ± s.d. from three independent experiments. $*P < 0.05$, $**P < 0.01$, $***P < 0.001$, two-way repeated measures ANOVA with a Tukey test in (C). Scale bars, 100 μm in (B) and (D).

Figure S3. The effect of AT7867 treatment on the induction of $HNF4\alpha^{+}$ primitive gut tube cells (PGTCs) into $PDX1^{+}$ cells. AT7867 treatment during this stage does not induce $PDX1^{+}$ cells. DMSO (white), AT7867 (black). Data are presented as the mean ± s.d. from three independent experiments. n.s., not significant, two-way repeated measures ANOVA with a Tukey test.

Figure S4. The effect of other AT7867 target inhibitors. (A-C) Dose response of AKT- (GDC-0068, AZD5363, MK-2206), RSK- (BI-D1870) and p70S6K- (PF-4708671) specific inhibitors (n = 1).

Figure S5. The effect of AT7867 on pancreatic endoderm differentiation in relation to cell density. (A) Representative flow cytometry plots showing co-expression of PDX1 and NKX6.1 in AT7867-treated cells. (B) Representative images of $PDX1^{+}NKX6.1^{+}$ cells from three independent experiments. Scale bar, 100 μm. (C) Fold change in cell number (Day 4/Day 0) at varying initial seeding densities. AT7867 treatment increased the cell number more than three-fold at all initial seeding densities. (D) The proportion of $PDX1^{+}NKX6.1^{+}$

cells at day 4. Although the cell number increased by more than three-fold, $PDX1^{+}NKX6.1^{+}$ cells were not induced at the lowest seeding density. (E) The proportion of $PDX1^{+}NKX6.1^{+}$ cells in S3 medium with or without AT7867. DMSO (white), AT7867 (black). Data are presented as the mean ± s.d. from three independent experiments in (C-E). $*P < 0.05$, $**P < 0.01$, $***P < 0.001$, n.s., not significant, two-way ANOVA with a Bonferroni test for multiple comparisons between treatments in (C) and (D), and two-way repeated measures ANOVA with a Tukey test in (E). Note that graph of DMSO overlaps with that of AT7867 in (E).

Supplemental tables

Table S1. List of antibodies used in this study.

Antigen	Species	Catalog #	Dilution
SOX17	Goat	AF1924, R&D Systems	1:200
HNF4α	Rabbit	sc-8987, Santa Cruz Biotechnology	1:200
PDX1	Goat	AF2419, R&D Systems	1:200
NKX6.1	Mouse	F55A12, University of Iowa	1:100
C-peptide	Rat	GN-ID4, University of Iowa	1:200
Glucagon	Mouse	G2654, Sigma-Aldrich	1:200
Ki67	Mouse	556003, Becton Dickinson	1:100
Ki67	Rabbit	NCL-Ki67p, Novocastra	1:1000
pHH3	Rabbit	3377s, Cell Signaling Technology	1:1000
pHH2AX	Rabbit	2577s, Cell Signaling Technology	1:200
Cleaved-Caspase3	Rabbit	9661, Cell Signaling Technology	1:200

Table S2. List of primer sequences used for qPCR.

Gene	Forward	Reverse
PDX1	AGCAGTGCAAGAGTCCCTGT	CACAGCCTCTACCTCGGAAC
PTF1A	CCCCAGCGACCCTGATTA	GGACACAAACTCAAATGGTGG
NKX6.1	ATTCGTTGGGGATGACAGAG	TGGGATCCAGAGGCTTATTG
GAPDH	GAAGGTGAAGGTCGGAGTC	GAAGATGGTGATGGGATTTC

Figure S1

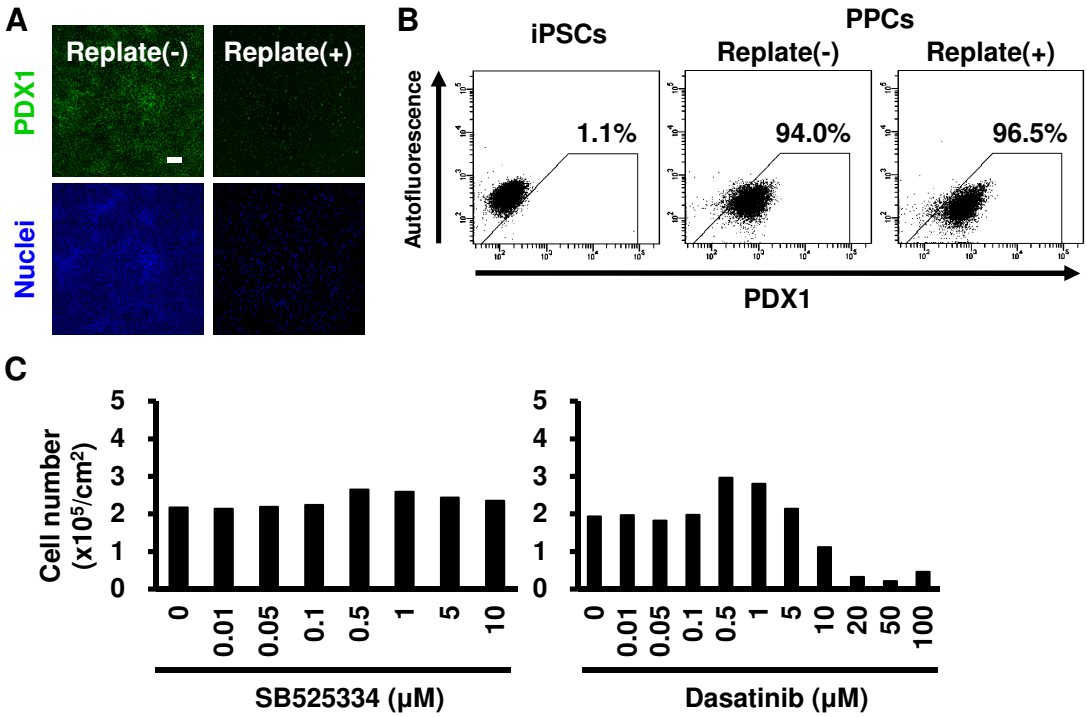
A
Replate(-)
Replate(+)
PDX1
Nuclei
B
iPSCs
PPCs
Replate(-)
Replate(+)
Autofluorescence
1.1%
94.0%
96.5%
PDX1
C
Cell number (x10^5/cm^2)
0
1
2
3
4
5
0
0.01
0.05
0.1
0.5
1
5
10
SB525334 (μM)
0
0.01
0.05
0.1
0.5
1
5
10
20
50
100
Dasatinib (μM)

Figure S2

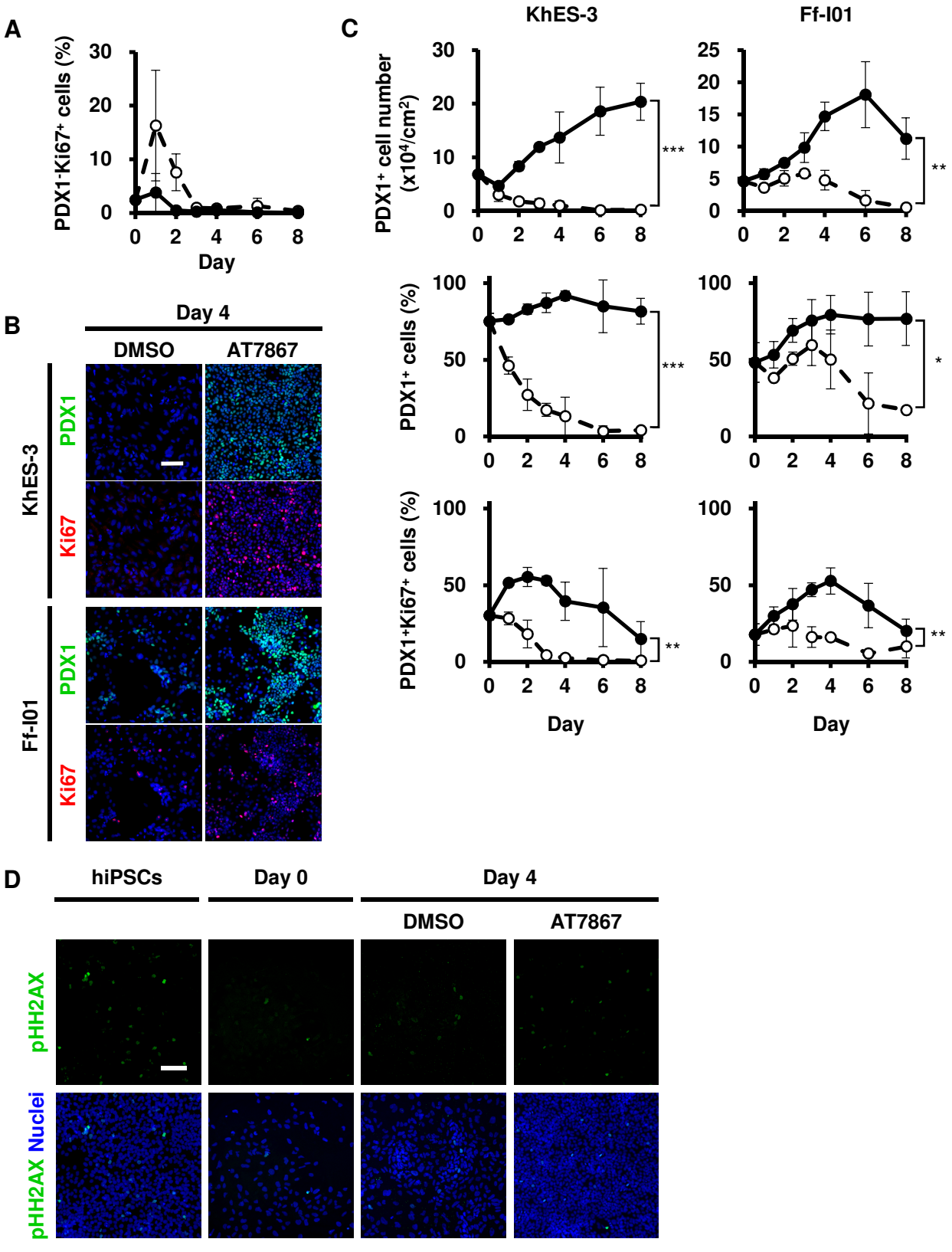
A
PDX1⁻Ki67⁺ cells (%)
Day
B
Day 4
DMSO
AT7867
KhES-3
Ff-I01
PDX1
Ki67
C
KhES-3
Ff-I01
PDX1⁺ cell number (x10⁴/cm²)
PDX1⁺ cells (%)
PDX1⁺Ki67⁺ cells (%)
Day
D
hiPSCs
Day 0
Day 4
DMSO
AT7867
pHH2AX
pHH2AX Nuclei

Figure S3

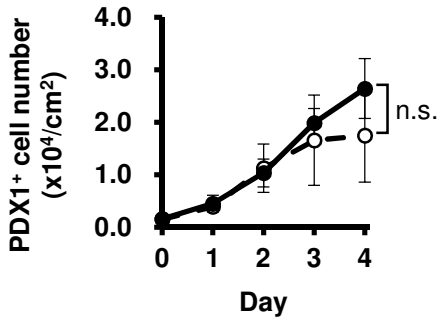

Figure S4

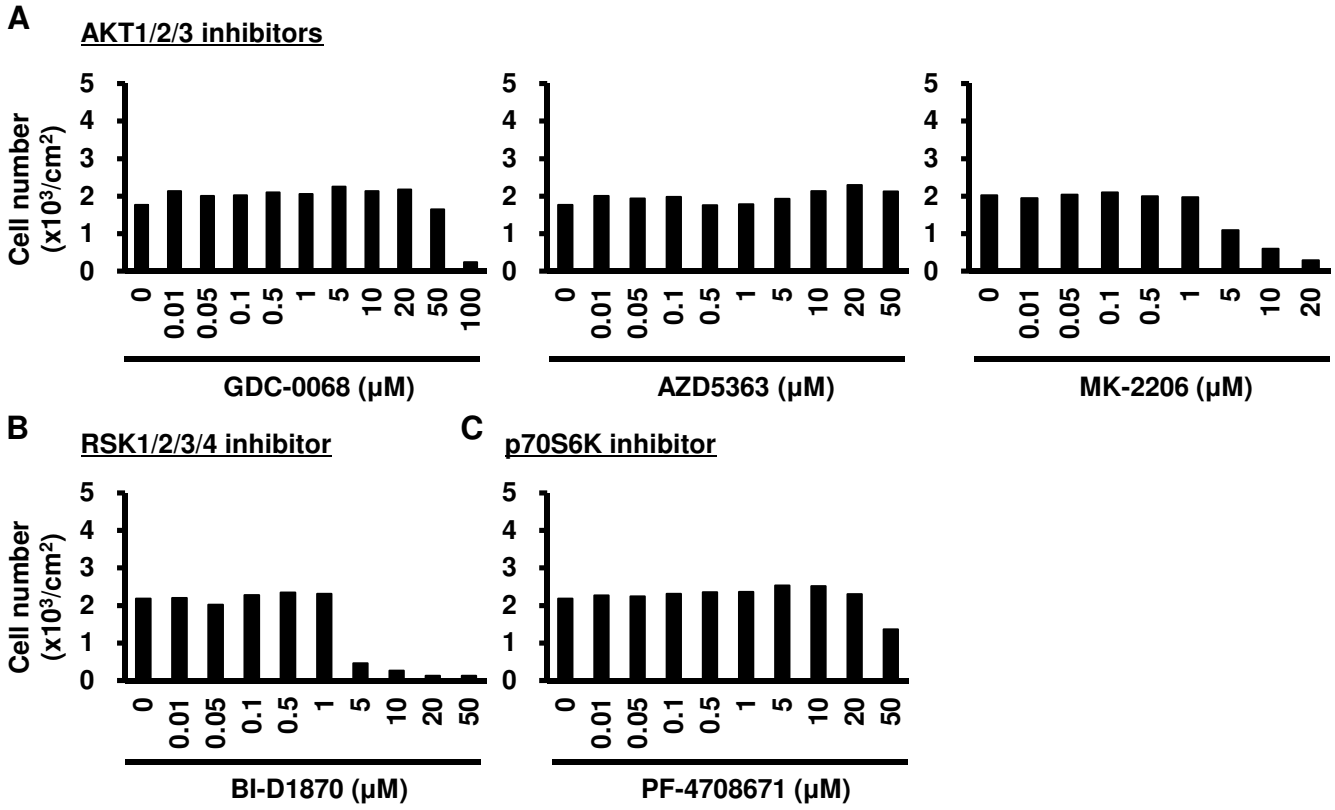
A
AKT1/2/3 inhibitors
Cell number (x10³/cm²)
0 1 2 3 4 5
0 0.01 0.05 0.1 0.5 1 5 10 20 50 100
GDC-0068 (μM)
0 0.01 0.05 0.1 0.5 1 5 10 20 50
AZD5363 (μM)
0 0.01 0.05 0.1 0.5 1 5 10 20
MK-2206 (μM)
B
RSK1/2/3/4 inhibitor
Cell number (x10³/cm²)
0 1 2 3 4 5
0 0.01 0.05 0.1 0.5 1 5 10 20 50
BI-D1870 (μM)
C
p70S6K inhibitor
0 1 2 3 4 5
0 0.01 0.05 0.1 0.5 1 5 10 20 50
PF-4708671 (μM)

Figure S5

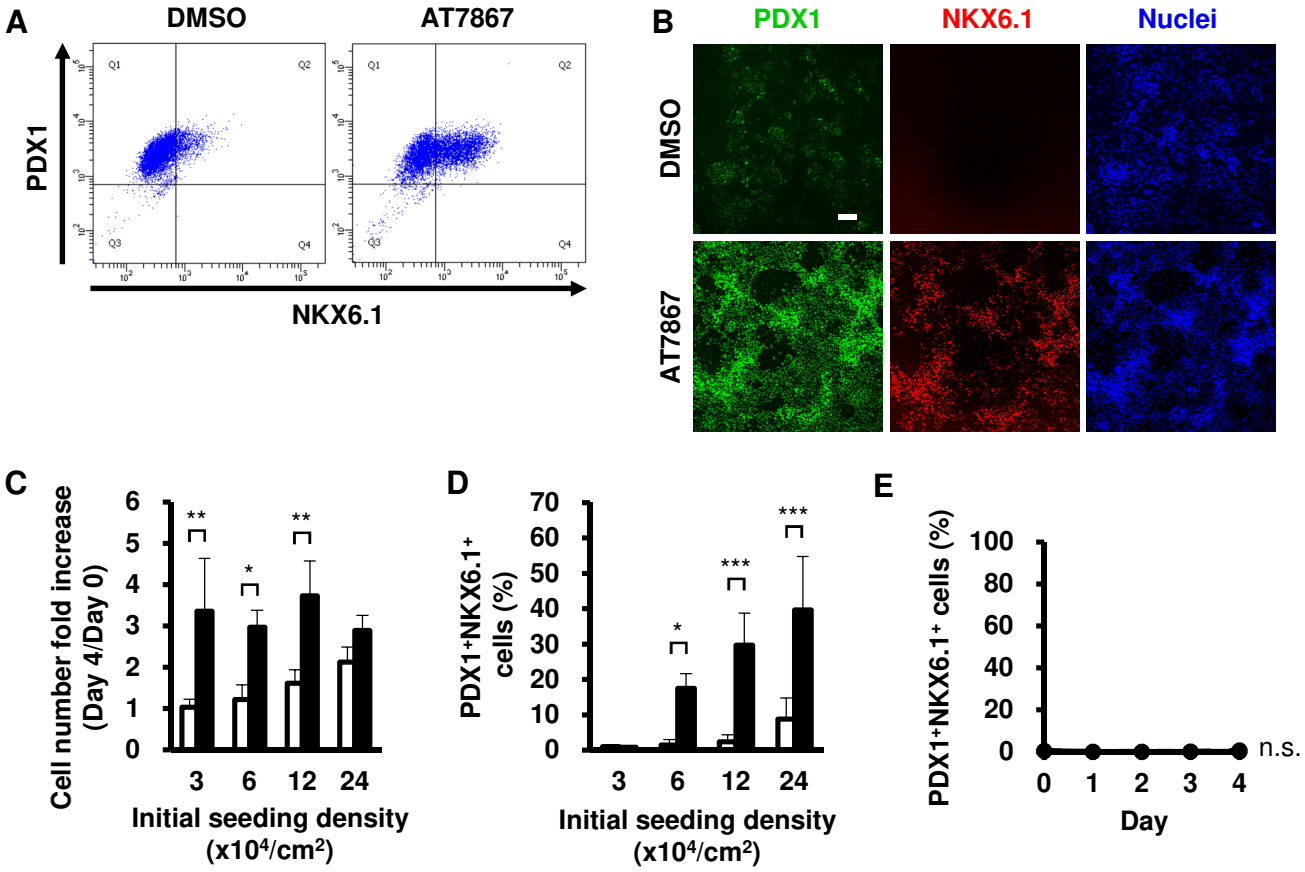
A
DMSO
AT7867
PDX1
NKX6.1
Q1
Q2
Q3
Q4
B
PDX1
NKX6.1
Nuclei
DMSO
AT7867
C
Cell number fold increase (Day 4/Day 0)
Initial seeding density (x10⁴/cm²)
D
PDX1⁺NKX6.1⁺ cells (%)
Initial seeding density (x10⁴/cm²)
E
PDX1⁺NKX6.1⁺ cells (%)
n.s.
Day